Single Fibre Swelling Behavior for Natural and Man-Made Cellulose Fibres Under Industrial Steeping Conditions

Xiang You (xiang.you@scitech.fi)
Scitech-Service Oy https://orcid.org/0000-0002-1456-1357
Feng Chen
ETH zurich
Yibo Ma
Aalto University
Annariikka Roselli
Metsa Spring Oy
Eric Enqvist
SciTech-Service Oy
Heikki Hassi
SciTech-Service Oy

Research Article

Keywords: Swelling, cotton, dissolving wood pulp, regenerated cellulose, cell wall

Posted Date: July 16th, 2021

DOI: https://doi.org/10.21203/rs.3.rs-689489/v1

Single fibre swelling behavior for natural and man-made cellulose fibres under industrial steeping conditions

Xiang You[1,*], Feng Chen[2,3], Yibo Ma[2], Annariikka Roselli[1,4], Eric Enqvist[1], Heikki Hassi[1,*]

[1] *Scitech-Service Oy, Helsinki, FI-00130, Finland*

[2] *Department of Bioproducts and Biosystems, School of Chemical Engineering, Aalto University, 00076 Aalto, Finland*

[3] *Wood Materials Science group, Institute for Building Materials, ETH Zurich, 8093 Zurich, Switzerland*

[4] *Metsä Spring Oy, Espoo, FI-02150, Finland*

* E-mail: xiang.you@scitech.fi, heikki.hassi@scitech.fi

Abstract

Swelling behavior of cotton, dissolving wood pulp (DWP), viscose staple fibre (VsF), and Tencel staple fibre (TsF) in varying sodium hydroxide (NaOH) were investigated by means of optical microscopy and were characterized by molecular mass distribution, X-ray diffractometer, and dynamic vapor sorption. Effect of temperature (20-45 °C) and duration (0-120 min) was studied. The results reveal that the swelling ratio of fibre in alkali solution depends on fibre accessibility and NaOH concentration. Among all the materials, VsF exhibited the highest swelling ratio and lowest swelling ratio has been observed for cotton fibre. The results suggest that the swelling is limited by the presence of plant cell wall structures in cotton and DWP, rather from fringed-fibrillar, semi-crystalline sub-structures, which result from the inherent tendency of cellulose molecules to form such structures during the biosynthesis of plant cell walls as well as during the formation of regenerated cellulosic textile fibre in wet-spinning.

Keywords: Swelling, cotton, dissolving wood pulp, regenerated cellulose, cell wall

Declarations

Funding

The financial support from Jenny and Antti Wihuri foundation (Grant No. 131219).

Conflicts of interest/Competing interests

The authors declare that they have no conflict of interest.

Availability of data and material

The authors declare that the data and material are available.

Code availability

Not applicable

Authors' contributions

Dr. Xiang You was responsible for the experimental design with Dr. Feng Chen and Dr. Annariikka Roselli, performed the experimental work, analyzed the corresponding results and wrote the manuscript as principal author, with copyediting by Dr. Feng Chen, Dr. Yibo Ma, and Dr. Heikki Hassi, under the supervision of Dr. Eric Enqvist and Dr. Heikki Hassi.

Additional declarations for articles in life science journals that report the results of studies involving humans and/or animals

Not applicable

Ethics approval

Not applicable

Consent to participate

The authors declare that they agree to participate.

Consent for publication

The authors declare that they agree to publication.

Introduction

Cellulose-based plant fibres are highly interesting sources of polymers for producing bio-based products. Native or derivatized cellulose has been used as a renewable resource in a wide variety of industries (Isogai and Atalla 1998; Cuissinat and Navard 2006, 2008). Cotton and technical celluloses (chemical pulps) are the main cellulose sources for industrial applications, for example, making paper, textile fibres and films (Klemm et al. 2005; Olsson and Westman 2013). However, as a non-thermoplastic polymer, the properties of cellulose prevent it from being processed for certain applications (Kihlman et al. 2012, 2013; Zhang et al. 2013).

Due to the high degree of crystallization and strong inter- and intramolecular hydrogen bonds, cellulose is relatively stable and is insoluble in water and many conventional solvents. Moreover, the hydrophobic interactions between the cellulose molecular sheets in the crystallite also restrict the dissolution of cellulose (O'Sullivan 1997; Nishiyama et al. 2002, 2003; Foress and Fremer 2003). Currently, only few solvents can directly dissolve cellulose (Gross and Chu 2010). The direct cellulose solvents can be classified into the system: aqueous media and non-aqueous media. Aqueous media consists of aqueous inorganic complexes (Cuam, Cuen), aqueous alkaline (NaOH), acids and molten inorganic salt hydrates ($ZnCl_2/H_2O$, LiSCN). Non aqueous media includes ionic liquids (ILs), organic solvent in presence of inorganic salts (LiCl/DMAc), DMSO/TBAF and amine oxide monohydrate (NMMO) (Heinze and Koschella 2005; Liebert 2010; Sen and Martin 2013; Olsson and Westman 2013). Of all direct solvents, only NMMO monohydrate is used as direct cellulose solvent on an industrial scale for spinning textile fibres (Lyocell process) (Chen et al. 2020).

The dissolution mechanisms of cellulose fibres in various direct solvents have been studied in detail. When native cotton fibres and wood fibres are placed in a certain swelling or dissolution agent, they show nonhomogeneous swelling. The solvent tends to first penetrate the Primary (P) cell wall through pores and dissolve the cellulose in the Secondary (S) cell wall. Since the cellulose chains are still trapped inside the fibre structure and the solvent penetration continues, due to osmotic pressure, the increasing solvent volume causes the expansion of the P cell wall (ballooning) (Cuissinat and Navard 2006; Le Moigne et al. 2010; Olsson et al. 2014; Mäkelä et al. 2018). According to the study of Cuissinat and Navard (2006), the behavior of DWP or cotton fibres in various solvent sytems (for example, NaOH-water or NMMO with 25 to 35% water) can be characterized by five particular modes: Mode 1) Accelerated dissolution by disintegration into cellulose fragments. Mode 2) Swelling in a large area by ballooning followed by dissolution. Mode 3) Large swelling by ballooning, but without dissolution. Mode 4) Homogeneous swelling without dissolution. Mode 5) No swelling and no dissolution. These modes reflect the quality of the solvents from excellent, moderate, weak, and non-solvent. In less powerful solvents ballooning may be followed by bursting of S1 and, then dissolution. (Cuissinat and Navard 2006; Zhang et al. 2013; Mäkelä et al. 2018; Chen et al. 2020). In the case of DWP fibres, the swelling of S2 layer of the S wall begins from the lumen (for example, filled with NaOH solution), ballooning occurs and generates tension to fibrils of P wall and S1 layer, which are less prone to swelling due to their more random fibril orientation. This tension further hinders the swelling of P and S1. P wall bursts and form collars that remain undissolved,

which locally prevent swelling of S wall. Finally, also S1 layer bursts and gets fragmented and dissolved in the form of aggregates. The same mechanisms apply to cotton fibres. However, cotton is considered more difficult to swell than wood pulp, which could be explained by the many sub-layers in its cell wall structure, with different direction of orientation (Klemm et al. 2005).

Various factors must be taken into account to understand fibre swelling and dissolution behavior: their chemical composition, properties of primary and secondary layers in natural fibres or properties of a skin in some man-made fibres, porosity, and cellulose crystallinity and molecular weight (Abu-Rous et al. 2006). For instance, viscose fibre has folded perimeter and a skin-core structure, due to immediate solidification of outermost fibre surface, under which there is a properly oriented skin layer. The core is poorly oriented, due to, i.e. the non-Newtonian flow of viscose dope through spinneret orifices. On the other hand, Lyocell fibre has a more uniform fibre structure because of slower solvent exchange between the fibre and the coagulation media.

To the best of our knowledge, there is no report comparing the swelling behavior of natural, chemical pulp, and man-made fibres, under the same conditions. In man-made cellulosic fibres (MMCFs) manufacturing processes, it's critical to avoid (usually microscopic) poorly swollen, unfragmented local domains of cellulose in the cell walls of the pulp. Therefore, the dynamics of the swelling and/or dissolution processes is of special importance.

This paper studies the swelling ratio and morphological changes of the structures of the single fibre and free-floating cellulosic fibres in different NaOH solution concentrations and temperatures. The behavior of cotton, DWP, VsF, and TsF with varying NaOH solutions conditions is observed by using optical microscopy. This work may contribute to the understanding of the cellulose swelling behaviors and the further work on the development of the viscose process. The aim is to identify sources of such defects (poorly swollen or undissolved, mostly microscopic residues) in spinning dope, which reduce the filterability or increase spinneret clogging rate in industrial MMCF manufacture.

Experimental methods

Materials

Raw cotton fibre without seed was obtained from Zhengzhou Share Machinery Co., Ltd, China. A commercially available DWP was obtained from Domsjö, Sweden. Two other man-made fibres VsF (1.3 DTEX, 39 MM, bright, raw-white) and TsF (1.3 DTEX, 38 MM, bright, raw-white) were donated by Lenzing, Austria. The characteristics of the fibres are presented in the Table 1. The solution was prepared by dissolve solid NaOH pallet in the milli-Q water to 5.5, 12, and 18% NaOH concentrations. All concentrations ratios are presented as % by weight (wt). All materials were cut into shorter length (fibre length $\leq$ 5mm) prior to the test.

Method

Molecular mass distribution (MMD) of cellulose fibres

MMD of the raw materials was determined by gel permeation chromatography. About 500 mg of the fibre sample was accurately weighted into a sample bottle. The samples were activated by a water–acetone-N,N-dimethylacetamide (DMAc) sequence. The activated samples (50 mg each) were dissolved in 90 g L^{-1} lithium chloride containing DMAc at room temperature and under gentle stirring. The samples were then diluted to 9 g L^{-1} LiCl/DMAc, filtered with 0.2 µm syringe filters, and analysed in a Dionex Ultimate 3000 system with a guard column, four analytical columns (PLgel Mixed-A, 7.5 x 300 mm) and refractive index (RI) detection (Shodex RI-101). Flow rate and temperature were 0.75 mL min^{-1} and 25 °C, respectively. Narrow pullulan standards (343–2,500 kDa, PSS GmbH) were used to calibrate the system. Number-average and weight-average molar mass, M_n and M_w, were calculated.

Determination of the crystallinity index by X-ray diffractometer (XRD)

XRD patterns of all macroscale cellulose fibres were collected in the transmission mode setting of an X-ray instrument (SmartLab, Rigaku) that was operated at 45 mA and 200 kV. All fibre samples were cut into debris and mounted on a multi-position sample holder. The Scans were performed in a 2 θ range between 5° and 60° by θ /2 θ mode.

The background profile was estimated under the same conditions, and it was subtracted from the obtained data. The crystallinity index (*CRI*) of fibres was estimated with the Segal method, using the intensity of crystal plane (I_{200}) at 2 θ = 22.7° and of amorphous parts ($I_{amorphous}$) at 2 θ = 18°:

$$CRI\ (\%) = 100 \times \left(\frac{I_{200} - I_{amorphous}}{I_{200}}\right) \quad (1)$$

Dynamic vapor sorption (DVS)

A DVS intrinsic apparatus (Surface Measurement system, London, UK)) with a measuring accuracy of 0.1 µg was used for water vapor sorption analysis. Around 10 mg of pre-dried grinded fibres were placed in the sample pan and preconditioned at a relative humidity (RH) of 0% at 25 °C until the equilibrium was reached using nitrogen (flow rate 100 $cm^3\ s^{-1}$). The adsorption cycle was performed in 0% RH steps to a maximum of 90% RH, and vice versa for the desorption cycle. In both cases, the RH was kept constant until a defined equilibrium condition was reached, for example, when sample mass change was below 0.001% per minute over 10 min. Then RH was increased to 90% and sample weight evolution and time to reach equilibrium (t_s) were recorded. For desorption the RH was decreased to 0%, and time to reach equilibrium (t_{des}) were recorded. Moisture sorption M_s (from M_0 to M_{90} at 90% RH) were calculated as follows:

$$M_s = \frac{M_{90} - M_0}{M_0} \times 100\% \quad (2)$$

Optical microscopy observations of fibre swelling

One single fibre was placed between two glass plates with the in-between distance around 140 µm controlled by spacers. The distance between two glass slides is much larger than the fibre's thickness. The ends of the fibre were fixed by tape and 1-2 drop of solvents added. Fibre diameter was recorded by a Zeiss Axio optical microscope in transmission mode equipped with a CCD camera (Metallux 3, Leitz) and Linkam TMS 91 hot stage to control temperature. The evolution of the fibre diameter in time t was calculated as D_t/D_0, where D_0 and D_t are initial diameter of the fibre at $t = 0$ and diameter of fibre at time t, respectively.

Results and discussion

Physico-chemical properties of cellulose fibres

Cotton is a natural cellulose fibre (cellulose content ~99%) with a complex morphology; its elementary fibre consists of more secondary (S) cell wall layers than wood fibre. The sub-layers of S wall are highly ordered and have a compact structure with the microfibril lying parallel to one another (Cuissinat and Navard 2006). DWP has special properties including high α-cellulose content (>90 % of dry matter) and relatively low molecular weight comparing to the cotton fibre (Mozdyniewicz et al. 2013). DWP is a raw material for man-made cellulosic fibre production. VsF is made via xanthantion of alkali cellulose made of DWP, followed dissolution and regeneration of the fibres by wet spinning in acidic coagulation bath. Due to the nature of the spinning, VsF consists of a dense skin and spongy core (Rous et al. 2006). On the other hand, TsF is made via direct dissolution in NMMO and spinning using Lyocell process. TsF has more homogeneous morphology, with a semipermeable skin, porous middle zone and dense fibre core (Rous et al. 2006, 2007).

To better understand the swelling behavior of the selected materials, a few physical properties of the material need to be characterized. The number-average (M_n) and weight-average (M_w) molecular weights of cellulose in each fiber are presented in Table 1, and the corresponding molar mass distribution are demonstrated in Figure 1a. The MMD of the raw cotton show a narrow distribution, and this is in accordance with what others have found for native cotton fibres (Timpa and Ramey 1989; Kleman-Leyer et al. 1992; Palme et al. 2014). Unlike cotton, DWP sample revealed subtle shoulder and high molecular weight peak indicating the presence of both low molar mass hemicellulose and relative long-chain cellulose. A distinct low molecular weight peaks for VsF and TsF are similar for all man-made fibres. It has to be noticed that cotton and VsF needed more time (2 weeks) to completely dissolve in LiCl/DMAc solution prior to the chromatographic analysis. The reason for cotton is due to high molecular weight andpossible reason for VsF is due to low accessibility caused by hornification.

The crystallinity of the material also governs their swelling behavior and it was analysed by XRD. The XRD patterns for the fibres are shown in Figure 1b. Cotton cellulose spectrum accordingly represents Cell-I, containing both crystalline and amorphous regions. Its Cell-I with crystallinity index of approximately 49.8%, which is typical for plant cellulose (Placet et al. 2012; Moryganov et al. 2018; Chen et al. 2020). DWP has slightly lower crystallinity comparing to cotton due to intensive

pulping procedure and present of the small amount of amorphous hemicellulose. The MMCFs demonstrate the Cell-II allomorph, as expected. The *CRI* is around 32.2% and 39% for VsF and TsF, respectively (Table 1). These results are in agreement with the previously reported crystallinity of MMCFs (Kreze and Malej 2003).

To compare the accessibility of the fibres, the dynamic water vapor sorption and desorption were measured. Moisture sorption (M_s), time to reach equilibrium t_s from 0 to 90% RH, and time to reach equilibrium t_{des} from 90 to 0% RH for each fibre are shown in Table 1. Cotton absorbs the least amount of vapor probably because of the "resistant" primary wall (Okubayashi et al. 2004; Xie et al. 2011) and higher cellulose crystallinity (*CRI* 49.8%). In the study of Abu-Rous (2006), cotton showed very small pores in the bulk of the fibre, but the drying cracks and flat pores between the sheets of the secondary wall appear as larger pores. Similar to the cotton fibre, the DWP also demonstrate relatively low vapour sorption due to the high crystallinity (*CRI* 45.8%). VsF absorbs the highest amount of moisture (M_s) due to its lowest crystallinity (*CRI* 32.2%) and wide pore size distribution from nanometre to micrometre scale (Okubayashi et al. 2005; Abu-Rous et al. 2006). Time to reach equilibrium, t_s = 1260 min, is the longest for VsF among the selected fibres probably could be explained by the hornification phenomena (Siroka et al. 2008) as viscose fibres may be overdried, and also because the absorption of a larger amount of vapor takes more time which related to its large surface area. TsF as one type of Lyocell fibre contains only nanopores in the bulk of the fibre with a slight gradient in pore density, and a very porous skin layer. As a result, TsF shows slightly lower moisture sorption than VsF. In the literature studies, cotton appears to absorb only little water; Tencel shows uniform water absorption over the whole fibre cross section and uneven water distribution was found in Viscose fibre (Abu-Rous et al. 2006).

Table 1. Characteristics of cellulose fibres.

Sample	M_n(kDa)	M_w(kDa)	*CRI*(%)	M_s(%)	t_s(min)	t_{des}(min)
Raw cotton	324	444	49.8	12.71	1113.1	1170.2
DWP	59	208	45.8	13.84	1260.1	1220.2
VsF	26	57	32.2	21.76	1674.8	2243.0
TsF	40	127	39	18.85	1497.4	1884.7

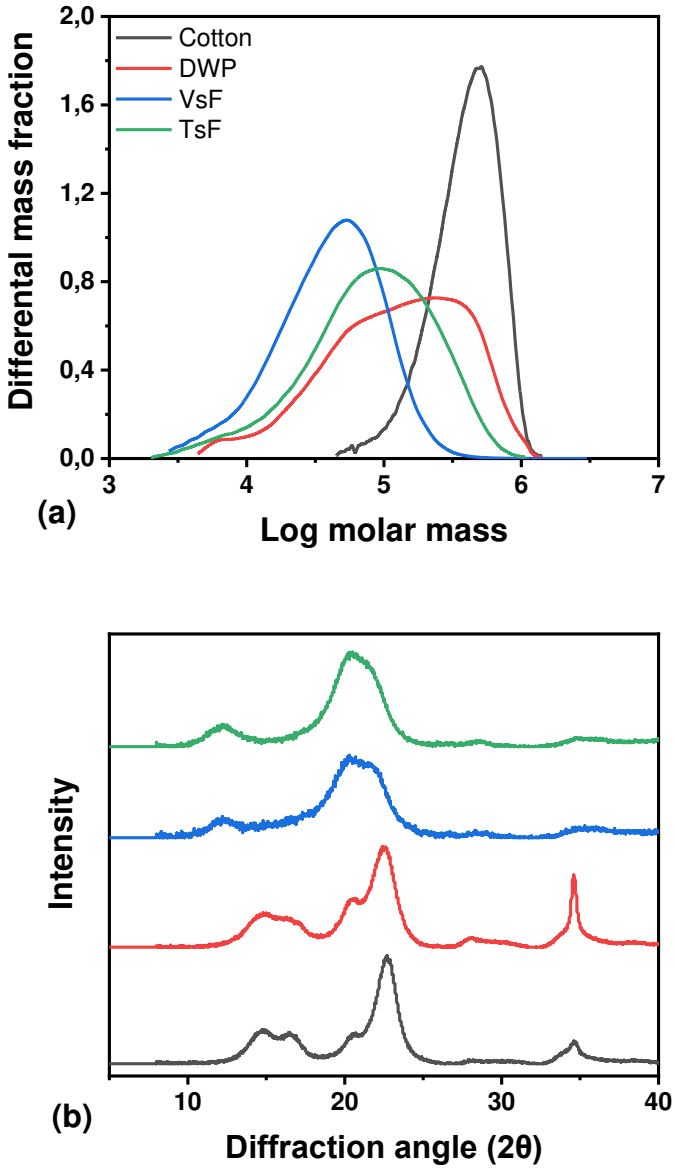

Figure 1. (**a**) Molecular mass distributions (MMD) and (**b**) X-ray diffraction (XRD) profiles of cotton, DWP, VsF and TsF

Fibre swelling behavior in NaOH solution

Cotton

As shown in Figure 2, dried cotton fibre collapses into a flattened bean-like cross section. It also twists along its length so that it looks like a twisted and flattened ribbon (Figure 2, 0 min). These twists are called convolutions: there are about 60 convolutions per centimetre (Dochia et al. 2012). In this study, the diameter of convolutions was measured to indicate the evolution of cotton fibre swelling ratio. The treatment temperature of 36 °C and 45 °C were chosen because they are close to the process conditions in the viscose process. Moreover, for viscose process, higher concentration

is necessary to ensure that the conversion to the alkoxide derivative proceeds to an acceptable extent. In industrial viscose process, typical NaOH concentration is around 17-19 wt%. (Cuissinat and Navard 2008; Wilkes 2011).

The images of cotton fibre evolution in NaOH solution at 45 °C are shown in Figure 2. Fibres show minor swelling, intermediate swelling, and swelling, in a 5.5, 12, and 18 wt% NaOH-water solvent in the selected conditions 45°, respectively. The swelling behavior of cellulose fibres in the relatively low NaOH solution indicates the weak solvating power. This may be reflected by the non-swelling/dissolution in amorphous state and crystalline region. When the cotton fibres are steeped in 12, and 18 wt% NaOH solution, cotton fibres loss of crystalline structure observed by the intermediate swelling and swelling phenomenon within 10 minutes. For all three NaOH solution concentrations, fibre swelling ratio kept constant after 10 minutes (Figure 3). The morphological changes of the cotton fibres at 45 °C are slightly higher comparing to that at 36 °C, swelling ratios 1.5:1.4, 2:1.7, 2.3:2 at 5.5, 12, and 18wt % concentrations, respectively. In industrial alkaline steeping conditions is generally performed at 30 – 55 °C.

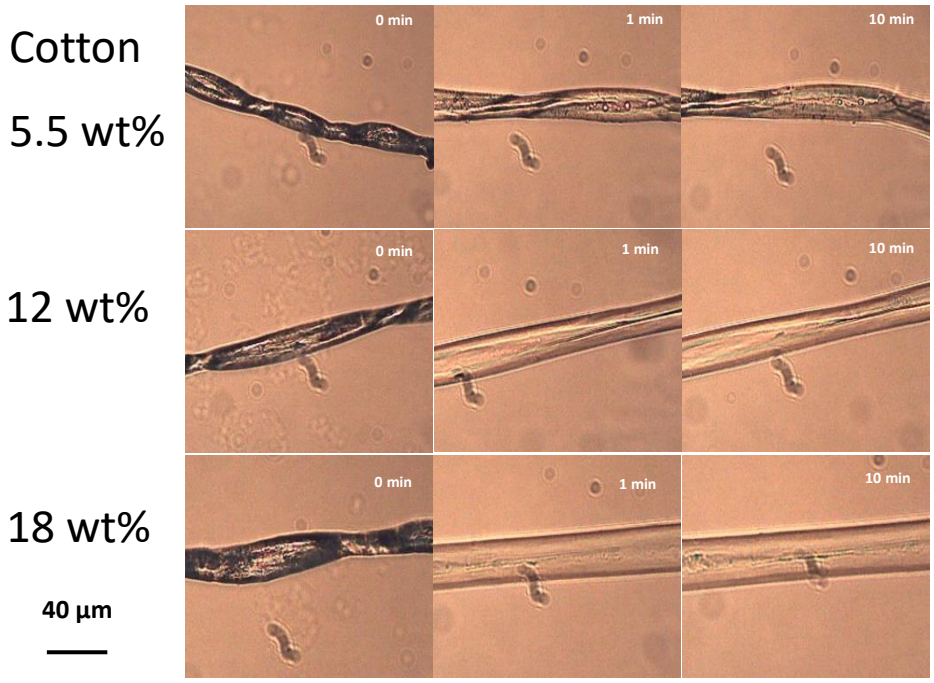

Figure 2. Optical microscopy images of cotton at 45 °C in 5.5, 12, 18 wt% NaOH solution.

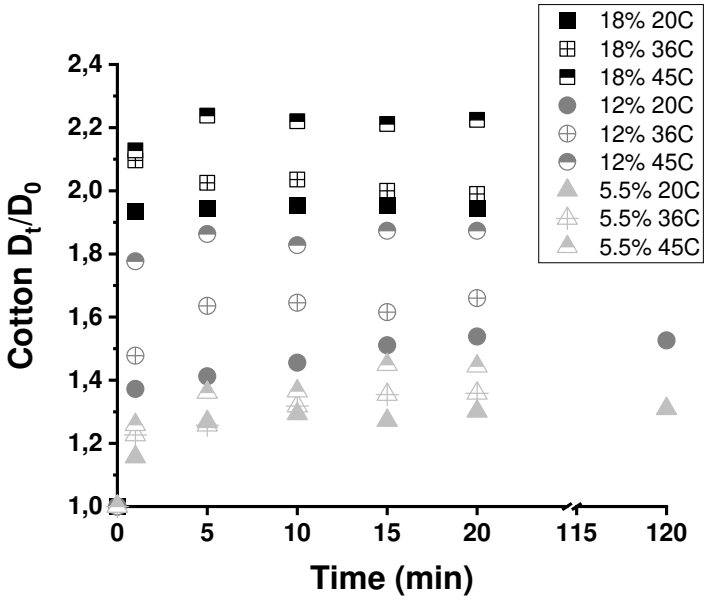

Figure 3. Evolution of cotton normalized diameter as a function of time.

Dissolving wood pulp

In the industrial scale viscose process, bleached dissolving wood pulp is typically the raw material and treated with steeping lye which contains a NaOH concentration of about 18 wt%. In this step and during the subsequent pre-aging, cellulose is converted into alkali cellulose for xanthation and its degree of polymerisation is adjusted to a level required for further processing (Mozdyniewicz et al. 2013). However, no suitable literature data are available for the swelling behavior of the DWP and the temperature and NaOH concentration ranges occurring during steeping of DWP. Therefore, this set of experiments describing the basis of DWP steeping, as a first step of viscose fibre manufacture.

Figure 4 presents the morphological changes of DWP fibres in 5.5, 12 and 18 wt% NaOH solutions at 36 °C. from the images, we have observed a pronounce increase in the fibre diameter and the inner layer of the fibre has been disintegrated at 12 wt% solution. DWP fibres steeped in both 5.5 and 18 wt% solution showed similar swelling behavior. At 20 °C and 36 °C (Figure 5) fibre swells more in 12 wt% NaOH solution in such relative low reaction temperatures, which had been confirmed in previous studies. This effect reflected that the solvating power of NaOH-water solution is governed by both NaOH concentration and treatment temperature. An increase in the temperature associated with too high or too low NaOH concentration decrease solvating power of the NaOH solvent. At higher temperature (45 °C), the NaOH-water solution dissolves more of the short-chain material. Some depolymerization also takes place during steeping, and the extent of this will increase with increasing temperature that eventually lead to partial dissolution of the pulp (Mozdyniewicz et al. 2013). This could be explained by the low DP of DWP which can be nearly fully dissolved, with few insoluble particles present.

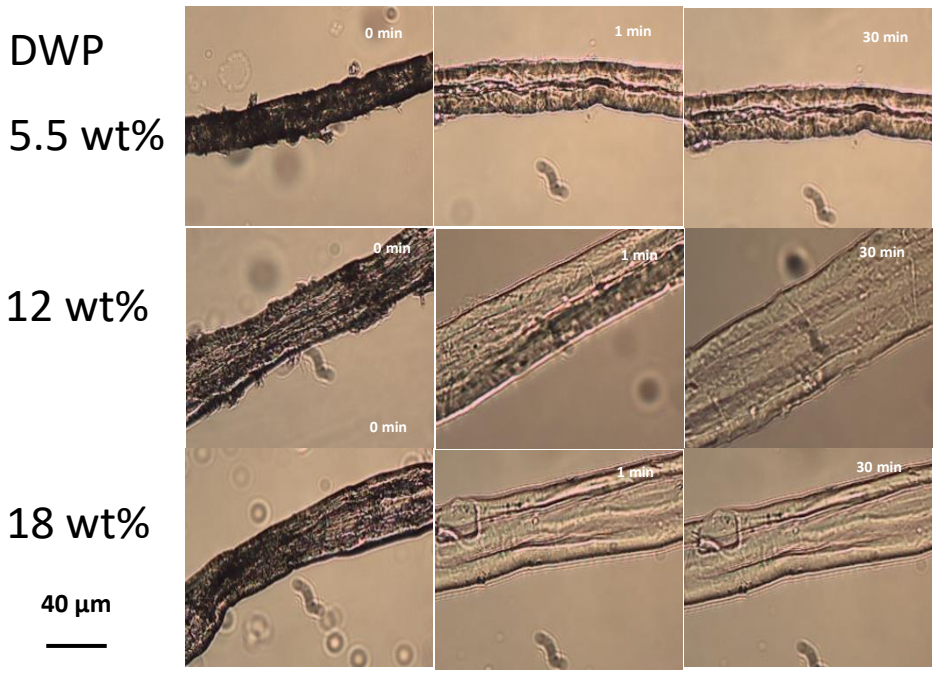

Figure 4. Optical microscopy images of DWP at 36 °C in 5.5, 12, 18 wt% NaOH solution.

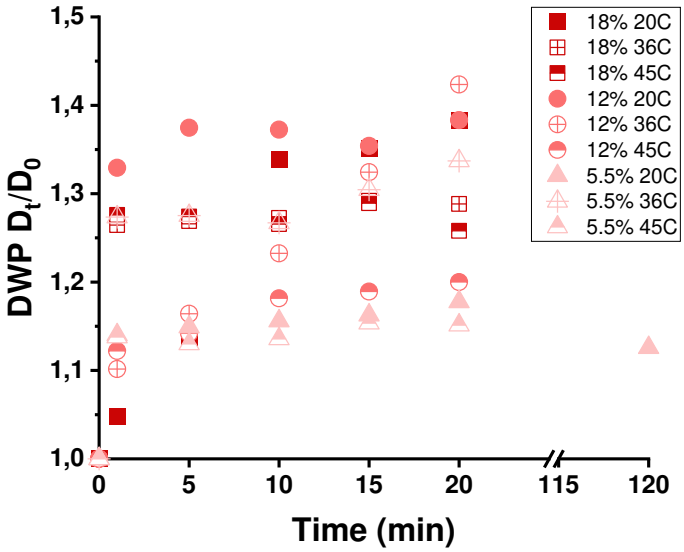

Figure 5. Evolution of DWP normalized diameter as a function of time.

Viscose staple fibre and Tencel staple fibre

Alkali treatment transforms the structure of native cellulose I of DWP and cotton into cellulose II. This transformation is generally known as mercerization. For regenerated fibres composed of cellulose II, the alkali treatment only increases the amorphous phase of the fibres (Rojo et al. 2013). The fibres swelling behavior upon the addition of the solvents at different temperatures are presented in Figure 6 and 7.

VsF and TsF fibre swell (Figure 6 and 7) more in 12 wt% NaOH solution, which is similar to DWP swelling those fibres swelling increase as the concentration is reduced. According to literature, pulp swelling to a maximum at around 11 wt% NaOH concentration (Wilkes, 2011). VsF and TsF swelling radially in a homogeneous way. These conditions increase the amorphous regions of the fibres and swell the microfibres and fibres. Fibre swelling ratio of viscose fibers were different from that of Tencel fibers, which was attributed to its inhomogeneous (skin-core) fiber structure compared to homogeneous fiber structure of Tencel fibers. The normalized diameter D_t/D_0 of fibres placed in NaOH is plotted in Figure 8 a,b as a function of time. VsF was swelling severe at 45 °C. In contrast, TsF was swelling severe at 20 °C.

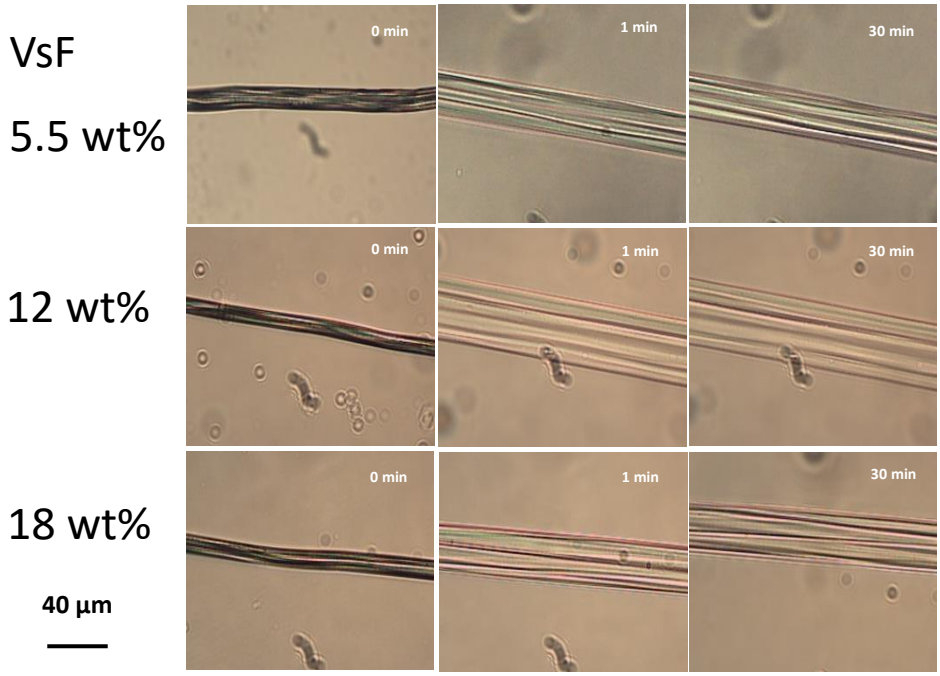

Figure 6. Optical microscopy images of VsF at 45 °C in 5.5, 12, 18 wt% NaOH solution.

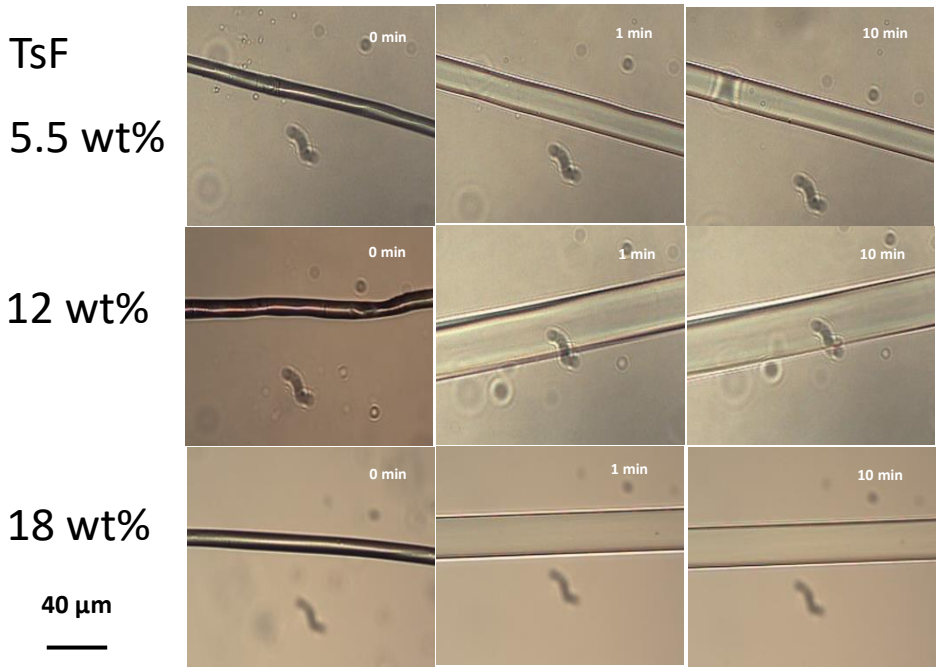

Figure 7. Optical microscopy images of TsF at 20 °C in 5.5, 12, 18 wt% NaOH solution.

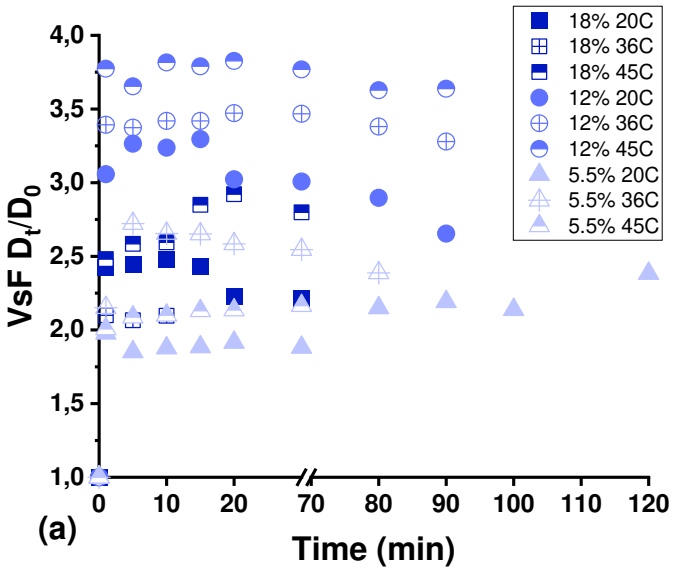

377

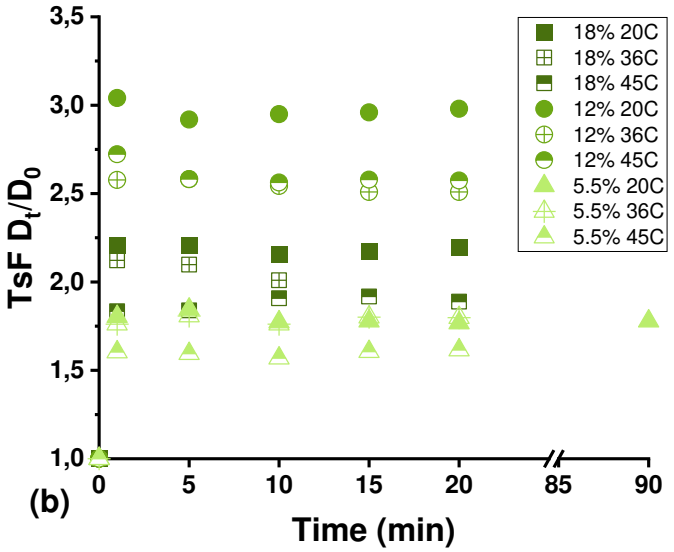

378

379 **Figure 8.** Evolution of (a) VsF, and (b) TsF normalized diameter as a function of time.

380

381 **The overall conversion in the viscose process**

382 The microfibrillar structure of a man-made cellulosic fibre resembles strongly the
383 original fibrillar structure of DWP cell wall layers. To make a spinning/processable
384 dope, we know that cellulosic spinning dopes are not molecularly dispersed systems.
385 They comprise ordered structures like fringed micelles, which tend to further aggregate
386 into larger structures. Therefore, the critical factor is not to dissolve better, what is
387 already properly dissolved, but to avoid poorly swollen, poorly dissolved domains of
388 cellulose (Schuster et al. 2003; Le Moigne 2008).

As the purpose of this study was to gain better understanding of the sources of poorly swollen and poorly dissolved residues in viscose spinning dope by comparing the swelling of cotton, DWP, VSF and TSF, the experimental conditions used in this study don't represent the real swelling behaviour during the steeping process with large scale. During the steeping stage of the viscose process, the raw material concentration is higher than suppresses the penetration of the liquor into the raw material due to the reduced solid to liquor ratio. On the other hand, the formation of the raw material also influences the swelling behaviour. In case of DWP, pulp sheet may be used instead of powders for steeping. The extreme compact structure and low surface area of the pulp sheet seriously lower the swelling rate of the cellulose. As for the raw material with long fibre format, the surface area of the material has also to be reduced by means of grinding in order to improve the penetration of the liquor into the materials. Grinding is also very important to avoid the accumulation of the fibres on the impeller which may lead to non-homogenous lye.

Conclusions

These results give good basis for more detailed identification of the sources and formation mechanisms of incompletely dissolved cellulosic particulates and gels in alkali-water based spinning dopes due to bad swelling. Such defects in spinning dopes are often the main factor limiting the production efficiency of viscose spinning lines and fibre quality. The results suggest that the swelling is limited by the presence of plant cell wall structures, which result from the inherent tendency of cellulose molecules to form such structures during the biosynthesis of plant cell. However, also other factors like hornification of fibres during drying may limit swelling.

Acknowledgments

The financial support from Jenny and Antti Wihuri foundation (Grant No. 131219) is gratefully acknowledged. Authors wish to thank Maija Nenonen and Sari Larmu for simulating industrial viscose process.

References

Abu-Rous M, Ingolic E, Schuster KC (2006) Visualisation of the fibrillar and pore morphology of cellulosic fibres applying transmission electron microscopy. Cellulose 13:411-419. https://doi.org/10.1007/s10570-006-9052-5

Budtova T, Egal M, Gavillon R, Gericke M, Heinze T, Liebert T, Roy C, Schlufter K, Navard P (2010) Comparison of Solution-State Properties of Cellulose Dissolved in NaOH/Water and in Ionic Liquid (EMIMAc). ACS Symp Ser 1033:179-196. https://doi.org/10.1021/bk-2010-1033.ch010

Budtova T, Navard P (2016) Cellulose in NaOH-water based solvents: a review. Cellulose 23:5-55. https://doi.org/10.1007/s10570-015-0779-8

Chen F, Sawada D, Hummel M, Sixta H, Budtova T (2020) Swelling and dissolution kinetics of natural and man-made cellulose fibres in solvent power tuned ionic liquid. Cellulose 27:7399-7415. https://doi.org/10.1007/s10570-020-03312-5

Cuissinat C, Navard P (2006) Swelling and Dissolution of Cellulose Part II: Free Floating Cotton and Wood Fibres in NaOH-Water-Additives systems. Macromol Symp 244:19-30.

https://doi.org/10.1002/masy.200651202

Cuissinat C, Navard P (2008) Swelling and dissolution of cellulose, Part III: Plant fibres in aqueous system. Cellulose 15:67-74. https://doi.org/10.1007/s10570-007-9158-4

Dochia M, Roskwitalski Z (2012) Cotton fibres. In: Kozłowski RM (ed) Handbook of Natural Fibres, Vol. 1. Woodhead Publishing, Cambridge, UK, pp 11-23

Foress KG, Fremer KE (2003) The nature and reactions of lignin - a new paradigm. Oy Nord Print Ab, Helsinki, pp 128

Gross AS, Chu JW (2010) On the molecular origins of biomass recalcitrance: The interaction network and solvation structures of cellulose microfibrils. J Phys Chem B 114:13333-13341. https://doi.org/10.1021/jp106452m

Heinze T, Koschella A (2005) Solvetns applied in the field of cellulose chemistry- a mini review. Polimeros 15:84-90. https://doi.org/10.1590/S0104-14282005000200005

Isogai A, Atalla R (1998) Dissolution of cellulose in aqueous NaOH solutions. Cellulose 5:309-319. https://doi.org/10.1023/A:1009272632367

Kihlman M, Aldaeus F, Chedid F, Germgård U (2012) Effect of various pulp properties on the solubility of cellulose in sodium hydroxide solutions. Holzforschung 66:601-606. https://doi.org/10.1515/hf-2011-0220

Kihlman M, Medronho B, Romano A, Germgård U, Lindman B (2013) Cellulose dissolution in an Alkali based solvent: Influence of additives and pretreatments. J Braz Chem Soc 24:295-303. http://dx.doi.org/10.5935/0103-5053.20130038

Kleman-Leyer K, Agosin E, Conner AH, Kirk TK (1992) Changes in molecular size distribution of cellulose during attack by white rot and brown rot fungi. Appl Environ Microbiol 58:1266-1270. https://doi.org/10.1128/aem.58.4.1266-1270.1992

Klemm D, Heublein B, Fink HP, Bohn A (2005) Cellulose: fascinating biopolymer and sustainable raw material. Angew Chem Int Ed 44:3358-3393. https://doi.org/10.1002/anie.200460587

Kreze T, Malej S (2003) Structural characteristics of new and conventional regenerated cellulosic fibres. Text Res J 73:675-684. https://doi.org/10.1177/004051750307300804

Le Moigne N (2008) Swelling and dissolution mechanisms of cellulose fibres. Doctoral dissertation, École Nationale Supérieure des Mines de Paris, pp 9-32

Le Moigne N, Jardeby K, Navard P (2010) Structural changes and alkaline solubility of wood cellulose fibres after enzymatic peeling treatment. Carbohydr Polym 79:325-332. https://doi.org/10.1016/j.carbpol.2009.08.009

Liebert T (2010) Cellulose solvents- remarkable history, bright future. Cellulose Solvents: For Analysis, Shaping and Chemical Modification. Publisher: Am Chem Soc Washington DC, pp 3-54. https://doi.org/10.1021/bk-2010-1033.ch001

Mäkelä V, Wahlström R, Holopainen-Mantila U, Kilpeläinen I, King A (2018) Clustered Single Cellulosic Fibre Dissolution Kinetics and Mechanisms through Optical Microscopy under Limited Dissolving Conditions. Biomacromolecules 19:1635-1645. https://doi.org/10.1021/acs.biomac.7b01797

Medronho G, Lindman B (2014) Competing forces during cellulose dissolution: From solvents to mechanisms. Curr Opin Colloid Interface Sci 19:32-40. https://doi.org/10.1016/j.cocis.2013.12.001

472 Moryganov AP, Zavadskii AE, Stokozenko VG (2018) Special features of X-ray analysis of cellulose
473 crystallinity and content in flax fibres. Fibre Chem 49:382-387. https://doi.org/10.1007/s10692-
474 018-9904-4

475 Mozdyniewicz DJ, Nieminen K, Sixta H (2013) Alkaline steeping of dissolving pulp. Part I: cellulose
476 degradation kinetics. Cellulose 20:1437-1451. https://doi.org/10.1007/s10570-013-9926-2

477 Nishiyama Y, Langan P, Chanzy H (2002) Crystal structure and hydrogen-bonding system in cellulose
478 Iβ from synchrotron X-ray and neutron fibre diffraction. Am Chem Soc 124:9074-9082.
479 https://doi.org/10.1021/ja0257319

480 Nishiyama Y, Sugiyama J, Chanzy H, Langan P (2003) Crystal Structure and Hydrogen Bonding System
481 in Cellulose Iα from Synchrotron X-ray and Neutron Fibre Diffraction. Am Chem So. 125:14300-
482 14306. https://doi.org/10.1021/ja0257319

483 O'Sullivan AC (1997) Cellulose: the structure slowly unravels. Cellulose 4:173-207.
484 https://doi.org/10.1023/A:1018431705579

485 Olsson C, Idström A, Nordstierna L, Westman G (2014) Influence of water on swelling and dissolution
486 of cellulose in 1-ethyl-3-methylimidazolium acetate. Carbohydr Polym 99:438-446.
487 https://doi.org/10.1016/j.carbpol.2013.08.042

488 Olsson C, Westmany G (2013) Direct dissolution of cellulose: background, means and applications.
489 Cellulose - Fundamental Aspects. Publisher: InTech., Rijeka, pp. 143-178.
490 http://dx.doi.org/10.5772/52144

491 Palme A, Idström A, Nordstierna L, Brelid H (2014) Chemical and ultrastructural changes in cotton
492 cellulose induced by laundering and textile use. Cellulose 21:4681-4691.
493 https://doi.org/10.1007/s10570-014-0434-9

494 Peng H, Dai G, Wang S, Xu H (2017) The evolution behavior and dissolution mechanism of cellulose in
495 aqueous solvent. J Mol Liq 241:959-966. https://doi.org/10.1016/j.molliq.2017.06.103

496 Placet V, Trivaudey F, Cisse O, Gucheret-Retel V, Boubakar ML (2012) Diameter dependence of the
497 apparent tensile modulus of hemp fibres: a morphological, structural or ultrastructural effect?
498 Compos Part A Appl Sci Manuf 43:275-87. https://doi.org/10.1016/j.compositesa.2011.10.019

499 Rojo E, Virginia Alonso M, Domínguez JC, Saz-Orozco BD, Oliet M, Rodriguez F (2013) Alkali treatment
500 of viscose cellulosic fibres from eucalyptus wood: Structural, morphological, and thermal
501 analysis. J Appl Polym Sci 130:2198-2204. https://doi.org/10.1002/app.39399

502 Rous MA, Ingolic E, Schuster KC (2006) Visualisation of the fibrillar and pore morphology of cellulosic
503 fibres applying transmission electron microscopy. Cellulose 13:411-419.
504 https://doi.org/10.1007/s10570-006-9052-5

505 Rous MA, Varga K, Bechtold T, Schuster KC (2007) A new method to visualize and characterize the
506 pore structure of TENCEL (Lyocell) and other man-made cellulosic fibres using a fluorescent dye
507 molecular probe. J Appl Polym Sci 106:2083-2091. https://doi.org/10.1002/app.26722

508 Schuster KC, Aldred P, Villa M, Baron M, Loidl R, Biganska O, Patlazhan S, Vavard P, Rüf H, Jericha E
509 (2003) Characterising the emerging Lyocell fibres structures by ultra small angle neutron
510 scattering (USANS). Lenzinger Berichte 82:107-117

511 Sen S, Martin J, Argyropoulos D (2013) Review of cellulose non-derivatizing solvent interactions with
512 emphasis on activity in inorganic molten salt hydrates. ACS Sustain Chem Eng 1:858-870.
513 https://doi.org/10.1021/sc400085a

514 Sixta H, Michud A, Haura L, Asaadi S, Ma Y, King A, Kilpeläinen I, Hummel M (2015) Ioncell-F: a high-
515 strength regenerated cellulose fibre. Nord Pulp Pap Res J 30:43-57.

https://doi.org/10.3183/npprj-2015-30-01-p043-057

Timpa JD, Ramey HH (1989) Molecular characterization of three cotton varieties. Text Res J 59:661-664. https://doi.org/10.1177/004051758905901105

Wilkes A (2011) The viscose process. In: Woodings C (ed) Regenerated cellulose fibres Vol. 1. The Textile Institute, Woodhead Publishing Limited, Cambridge, pp. 37-61

Zhang S, Wang W, Li F, Yu J (2013) Swelling and dissolution of cellulose in NaOH aqueous solvent systems. Cellul Chem Technol 47:671-679